An experimental study on the design method of a real-sized Mobile Bridge for a moving vehicle

Y. Chikahiro[1], I. Ario[1], M. Nakazawa[2], S. Ono[3], J. Holnicki-Szulc[4], P. Pawlowski[4] & C. Graczykowski[4]
[1]*Department of Civil and Environmental Engineering, Hiroshima University, Japan*
[2]*Department of Civil and Environmental Engineering, Tohoku Gakuin University, Japan*
[3]*Japan Construction Method and Machinery Research Institute, Japan*
[4]*Department of Intelligent Technologies, Institute of Fundamental Technological Research, Poland*

Abstract

Many natural disasters can cause not only a critical situation in local resident's lives and facilities but also significant damage to the economy. Although we have to undertake quick rescue actions for these damages, there are many recovery problems, due to the occurrence of secondary disasters at each rescue worksite. Looking at previous studies of deployable structures and the control regulation of the multi-folding micro-structure, we propose a new type of foldable bridge, with a scissors structure called the Mobile Bridge™. In this paper we discuss vehicles passing a test on a real-scaled Mobile Bridge, so as to evaluate its mechanical characteristics and application limits. Moreover, we verify the compatibility amongst the results of the analysis, the calculations and the experimental values by means of a theoretical approach and method. From these results, if design of Mobile Bridge is simplified, we understood that it is sufficient to treat the load as equivalent nodal force applying the pins without the stiffness of the deck..
Keywords: Mobile Bridge™, scissors type of emergency bridge, aluminium alloy materials, vehicle loading test.

WIT Transactions on The Built Environment, Vol 136, © 2014 WIT Press
www.witpress.com, ISSN 1743-3509 (on-line)
doi:10.2495/MAR140081

1 Introduction

In recent years, the world has seen many kinds of natural disasters, such as earthquakes, floods and tsunamis. In the case that we are investigating – a very large flood along several branches of the Yamakuni River in Kyushu, northern Japan, 2012 – a lot of areas suffered from bridge and road damage. Therefore, the designers or engineers of bridges have to consider how to rebuild a damaged infrastructure and how to build a new type of rescue system, which can be implemented quickly, because rescue time is very important when trying to save lives after an emergency.

From a previous study on the optimization structure and deployable structure of bridges [1–4], we propose a new type of emergency bridge by the name of the Mobile Bridge™ (MB), which can be expanded and stored for concrete disaster recovery system [5]. Although the upper and lower chord members of a bridge are main elements, which resist the bending moment in a general truss bridge, the MB can be built using a scissors mechanism for a bridge formation and resist sectional force in spite of lacking the one member [6–9].

A scissors structure, which is applied to the structural form of an MB, is typically a deployable structure that has good storage and conveyance performance and is thusly named because its structural form combines the member in the shape of scissors. The joint that connects the member of scissors is named a pin-junction, which is joined by a flexible hinge and the pin joining section is called a "pivot", which exists in the central portion of a scissors member intersect. The advantages of this structure are as follows: 1) Even if there are few members for the construction of the scissor structure, its deployment and storage can be performed quickly, 2) its assembly, conveyance, and demolition is easy and 3) because the scissors structure can deploy and store all units by one control force, if the flexibility increases, its deployment performance is highly efficient and more useful.

In this paper, we discuss the vehicles passing a test on the real-scaled Mobile Bridge (called MB1.0) in order to evaluate its mechanical characteristics and application limits for scissors type of bridge. Moreover, we verify the compatibility amongst the results of the analysis, the calculations and the experimental values by means of a theoretical approach and method.

2 Outline of the real-scaled Mobile bridge

The schematic view of the experimental, two-unit scissors model for a real-scaled mobile bridge (MB1.0) on which vehicles can load is shown in Figure 1. When deployment starts, the member gradually slopes and the span is extended. Moreover, because the deck is sated in MB1.0, the deck works with the member as deployment progresses. Following this, the scissors deployment angle is at an angle of 60 degrees. The total length of the span is 7.0 m and the height is 2.0 m. The total weight, considering the structural parts, such as the main member, the shaft and the pin of the bridge, is 8.4 kN. The aluminum alloy component of the three-room hollow section, which uses A6N01 material, is

used for the main member, the surrender bending moment is 20.1 kNm and the ultimate bending strength is 39.9 kNm. The deck on which the vehicles travel (hereafter called the aluminum alloy deck) consists of an A6063 extrusion section. Only a portion of the aluminum alloy deck was constructed – the section upon which the wheel loads act – because of weight saving. Moreover, the deployment action aims at shortening the construction time by uniting and interlocking the scissors member and the aluminum alloy deck. The A6N01 material is E = 61.0 GPa, σ_B = 198.8 MPa and σ_y = 180.0 MPa, while the A6063 material is E = 68.0 GPa, σ_B = 150.0 MPa and σ_y = 110.0 MPa.

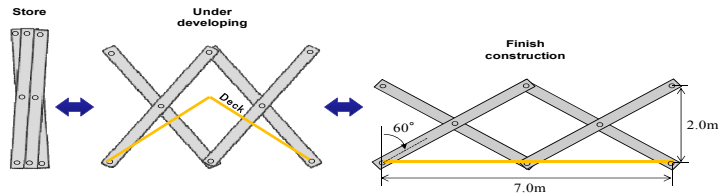

Figure 1: The stretching behavior of MB1.0.

3 Theory of scissors mechanism

3.1 The mechanics of a unit scissors structure

A Free Body Diagram (called FBD) for a unit of scissors structure is shown in Figure 2. When the length of the members is L_0 and the angle of inclination is θ, the sectional length λ and the height $2h$ are L_0s in $\theta = \lambda$ and $L_0\cos\theta = 2h$. So, the construction and storage of such a structure can be shown by the angle θ. This unit scissors structure can be designed by using the equation of equilibrium. The equation of equilibrium concerning each of the external forces $V_A - V_E$ and $H_A - H_E$ is given as the following two expressions;

$$\sum H = H_A + H_B + H_C + H_D + H_E = 0, \tag{1}$$

$$\sum V = V_A + V_B + V_C + V_D + V_E = 0 \tag{2}$$

Looking at the members AE and BD, the intersect is shown in Figure 3. It is calculated that the two equilibrium equations of moments occur at Point C, as in the following;

$$\text{Member of AE: } M_C = -hH_A + \frac{\lambda}{2}V_A = -hV_E + \frac{\lambda}{2}V_E, \tag{3}$$

$$\text{Member of BD: } M_C = hH_B + \frac{\lambda}{2}V_B = hV_D + \frac{\lambda}{2}V_D \tag{4}$$

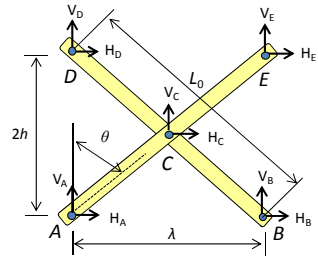

Figure 2: FBD of a unit scissors structure.

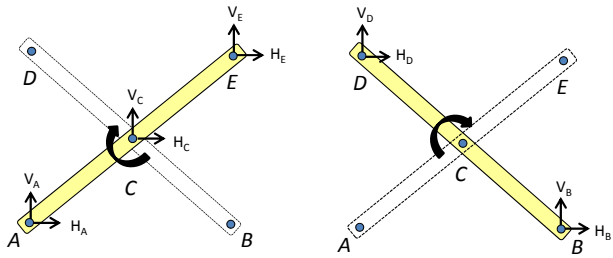

Figure 3: Continuity conditions of each member.

Let us now consider the case of the cantilever model, which has a pinned support for point A and point D. It is possible to use a matrix by arranging the four calculated equilibrium equations eqn (1)–eqn (4), as shown in eqn (5);

$$\begin{bmatrix} 1 & 0 & 1 & 0 \\ 0 & 1 & 0 & 1 \\ -2h & \lambda & 0 & 0 \\ 0 & 0 & 2h & \lambda \end{bmatrix} \begin{Bmatrix} H_A \\ V_A \\ H_D \\ V_D \end{Bmatrix} = -\begin{bmatrix} 1 & 0 & 1 & 0 \\ 0 & 1 & 0 & 1 \\ 0 & 0 & 2h & -\lambda \\ -2h & -\lambda & 0 & 0 \end{bmatrix} \begin{Bmatrix} H_B \\ V_B \\ H_E \\ V_E \end{Bmatrix} - \begin{Bmatrix} H_C \\ V_C \\ 0 \\ 0 \end{Bmatrix} \tag{5}$$

Similarly, we can get equilibrium as eqn(6) in the simple beam model, which has a pinned support for point A and point B;

$$\begin{bmatrix} 1 & 0 & 1 & 0 \\ 0 & 1 & 0 & 1 \\ -2h & \lambda & 0 & 0 \\ 0 & 0 & 2h & \lambda \end{bmatrix} \begin{Bmatrix} H_A \\ V_A \\ H_B \\ V_B \end{Bmatrix} = -\begin{bmatrix} 1 & 0 & 1 & 0 \\ 0 & 1 & 0 & 1 \\ 0 & 0 & 2h & -\lambda \\ -2h & -\lambda & 0 & 0 \end{bmatrix} \begin{Bmatrix} H_D \\ V_D \\ H_E \\ V_E \end{Bmatrix} - \begin{Bmatrix} H_C \\ V_C \\ 0 \\ 0 \end{Bmatrix} \tag{6}$$

From the above results, unknown reaction forces can be obtained by considering the loading condition and the boundary condition for these.

3.2 Mechanics of a scissors structure in the consideration of deck

Next, let us consider the mechanical model when adding the deck to the fundamental theory of the scissors structure, as discussed in the previous section. The unit scissors model with the deck is shown in Fig. 4(a), and the FBD, which is made of the unit scissors and each independent deck, is shown in the Fig. 4(b). Figure 4(a) shows the whole of the structure with a moving load, such as a vehicle. A vehicle passes over the deck between nodes *A* and *B*. According to the wheel load, the reaction forces on the supports occur in the deck, as shown in Figure 4(b). The reaction force that arose in the deck is transmitted to the main member of a scissors unit, as an external force, *P*1 and *P*2. Because the wheel load transmitted from the deck changes with wheel positions, it is thought that the stress distribution, which occurs in the scissors member and the deck, changes depending on the position of the vehicles.

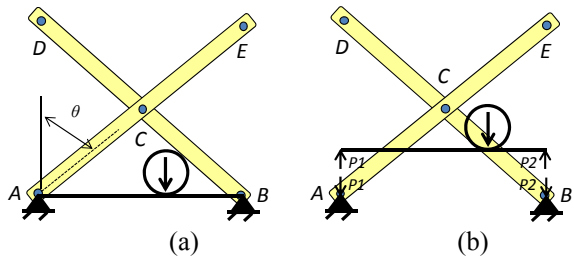

Figure 4: FBD of a unit scissors structure with deck. (a) Whole system, (b) FBD of the deck.

4 Experimental evaluation for the load-carrying capacity of the aluminium alloy deck

This section describes the bending fracture experiment and its results in order to check for the safety of the aluminum alloy deck under vehicle loading.

4.1 Outline of the aluminum alloy deck

Figure 5 shows the aluminum alloy deck with a vehicle traveling. The length of the deck is 3200 mm with a width of 500 mm. The quality of the material is A6063-T5 and is formed by welding two types of hollow extrusions together; one with a width of 200 mm and the other with a width of 100 mm. The weight of one panel is 490N.

4.2 Experimental conditions

The aluminum alloy deck was created by setting a steel pipe of φ = 20 mm to both ends of the pin fixing part. The loading plate, which supposes a tire contact area, uses a 175 mm × 175 mm steel plate and a rubber board for prevention, consulting the Eurocode for bridge designs.

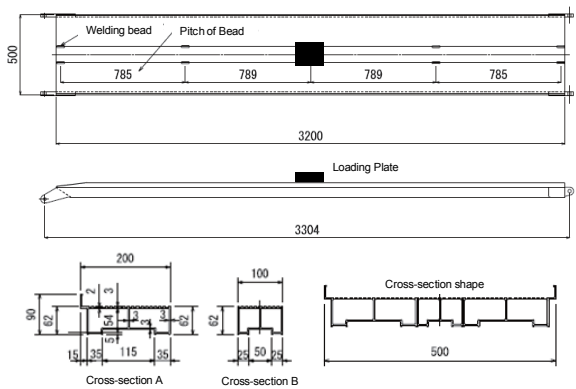

Figure 5: Schematic diagram of the deck.

4.3 Experimental results

The load-displacement curve at the loading point is shown in Figure 6. The horizontal axis shows the displacement of the head part of the loading machine and the vertical axis shows the increment of the load. Until $P = 1$ kN, the load is increased by 0.2 kN and after $P = 1$ kN, the load increases by 1 kN until $P = 14$ kN. After observing $P = 14$ kN, the load was removed and the residual displacement and strain on the aluminum alloy deck was checked. Then, the displacement was increased by $\delta = 10$ mm. The aluminum alloy deck lost its bearing force, showing a maximum load of 15.1 kN and the experiment ended.

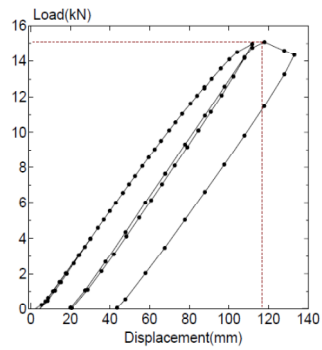

Figure 6: Load–displacement curve.

4.4 Distribution of the stress in the central cross-section position

The stress distribution in the central section is depicted in Figure 7 at the times of $P = 4.5$ kN, 5.0 kN and 5.5 kN. The stress values (MPa) are shown on the vertical axis and the distances (mm) from the neutral axis are shown on the horizontal axis. Moreover, the line of $\sigma_y = \pm 110$ MPa shows the yield stress

of the quality of the material A-6063. From Figure 7, we can see that the undersurface first surrendered at the time of P = 5.0 kN. So, the serviceability limits for the load of the deck was as much as 5.0 kN. At this time, the maximum bending moment was M_{max} = 28.7 kNm in the central part of the aluminum deck and this value yielded the bending moment for the deck.

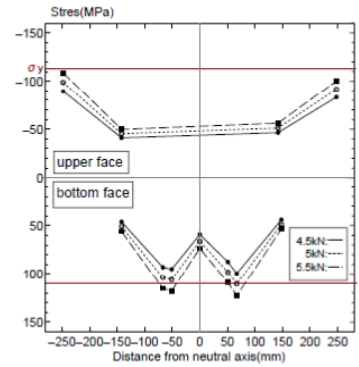

Figure 7: Distribution of the strain values at central section of the deck.

5 The vehicle loading test using MB1.0

In this section, the outlines and results of the vehicles loading test using MB1.0 are described. Moreover, the experimental results are compared with an equilibrium elastic theory of scissors and FE analysis.

5.1 Vehicles outline

Two kinds of vehicles – a Honda STREET and a Nissan AD van – were used for the vehicles loading test. The STREET's (full length*full width*overall height) was (3195 mm*1395 mm*1870 mm), while the AD van's (full length*full width*overall height) was (4370 mm*1895 mm*1510 mm). The wheel base of the STREET was 1900mm and the total weight of the STREET concluding a driver is 9.6kN distributed 5.2kN of front axial and 4.4kN of rear axial. The wheel base of AD van was 2535mm and the total weight of the AD van concluding a driver is 13.8kN distributed 7.5kN of front axial and 6.3kN of rear axial.

5.2 Vehicles stop position and loading condition

From Table 1, it can be seen that the measurement was performed five times. When the front wheel, the axle (that is defined here as the intermediate part of the front and the rear wheel) and the rear wheel came to a specific point and stopped and the value of the strain was measured. The stop positions were at the center of the deck for the first unit scissors and the central part of MB1.0. Two cases of loads were used, as seen in Table 2. One case depicts the STREET,

which is a light vehicle and the other case depicts the AD van, which is a standard-sized car. In loading Case 2, the additional weight was loaded from Case 1 the backseat of the vehicles and ran.

Table 1: Loading conditions.

Load case	Type of vehicle	Loading condition(kN)		
		Total	Front axis	Rear axis
1	STREET	9.6	5.2	4.4
2	AD Van	13.8	7.5	6.3

Table 2: Vehicles stop positions.

Case	Vehicle stop position	
A	Front wheel	Center of first slab
B	Wheel axis	Center of first slab
C	Front wheel	Center of MB1.0
D	Wheel axis	Center of MB1.0
E	Rear wheel	Center of MB1.0

5.3 Verification of the frame analysis

We analyzed MB1.0 by Autodesk Inventor. The analysis was possible by using internal programming (ANSYS) which was interlocked in the CAD. To identify all the elements, a beam element was used. The analysis was done by paying attention to the Pattern *D*, in which the maximum strain occurred with the vehicles in the stop position.

The analysis models are shown in Figure 8. The dead load consists of the main member, the shaft, and the deck. Figure 8 (a) is the strict model considering the deck and Figure 8 (b) is the simple model not considering the deck. The strict model made the wheel load on the deck, which acted on the wheel position after vehicle loading acted on the floor version, as shown in Figure 8 (a). The simple model made the wheel load on the pin, whose member intersects in the way of an equivalent nodal force, as seen in Figure 8 (b). The live load, as depicted by the red arrow acts according to the wheel load and the yellow arrow depicts the equivalent nodal force. As a boundary condition, the shaft part of both ends is fixed into the pin fixation in a simple beam state.

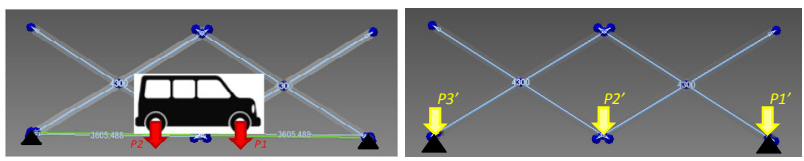

(a) (b)

Figure 8: 2D analytical model: (a) Strict model, (b) simple model.

5.4 Results of the experiment

Figure 9 (a) and (b) shows the strain distribution when the vehicle was loaded in the center of the bridge. Figure 9 (a) portrays a member, which stands in a row like a type of mountain from the supports and Figure 9 (b) pays attention to the member, which is in a free-state and the target is colored in red. Moreover, the blue mark in the figure shows the position of the strain gage. It can be seen that the experimental and analytical values are less than the allowance strain (= 2000 με) for loading vehicles from up until 13.3 kN. A maximum strain of about 500 με occurred in the member intersection part, so there was a safety ratio of nearly double that of the yield strain.

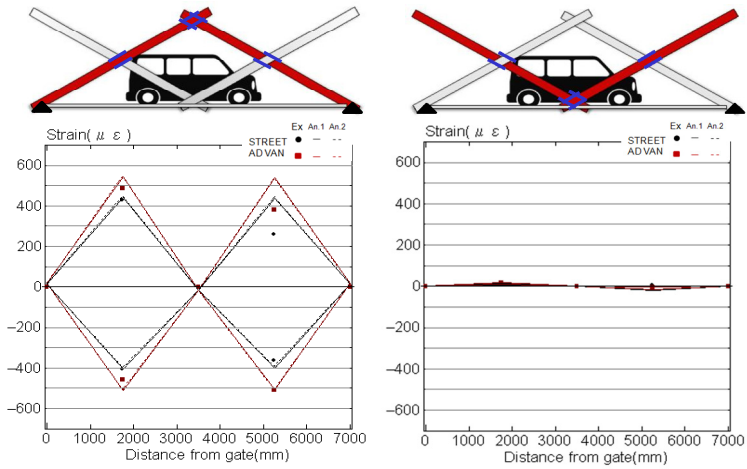

Figure 9: Distribution of strain in the central MB1.0: (a) Member ends-supports, (b) member ends-free.

From Fig. 9 (a) we can see that the maximum strain was measured at 500 με by the circumference of the pivot of the first unit and the minimum strain was measured by the circumference of the pivot of the second unit. . Because the distribution of the strain almost equaled in the compression and the tension area, it turned out that the member's influence on the bending moment was great. Although accuracy had variations in comparison with the analytical results, the maximum value was distributed within 10%.

Fig. 9 (b) shows that hardly any strain from the member occurred around ± 10 με, which was in an end-free state. It turned out that the analytical results also showed the same tendency and the bending moment did not act on the member, but the strain rose with a little axial tension.

6 Conclusion

The points which became clear from this research are followed as:

1) Through the bending test, it was proven that the load-carrying capacity of an aluminum deck is sufficient for vehicles to pass over it.
2) In the static loading experiment, it was found that the strain change arose in MB1.0 at the time of the vehicles loading and it was consistent with an analytical value of less than 10%.
3) With a maximum loading weight of 13.8 kN, the main member and decks are within allowable stress, and it turned out that the vehicles of about 10 kN could pass safely.

Acknowledgements

This research was supported for Dr. I. Ario by a Grant-in-Aid-Scientific-Research Base Research (B) of JSPS in 2011 – 2013. We appreciated that all experiments were supported by Japan Construction Method and Machinery Research Institute. Moreover, we appreciate that a sample of the aluminum materials were offered by Star Light Metal Industry Co., Ltd. in Japan.

References

[1] J. Holnicki-Szulc, P. Pawlowski and M. Wiklo: High-performance impact absorbing materials – the concept design tools and applications, Smart Materials and Structures: Int. J. Non-Linear Mechanics, pp. 461–467, 2003.

[2] I. Ario and A. Watson: Structural Stability of Multi-Folding Structures with Contact Problem: *Int. J. Non-Linear Mechanics*, Vol. 324 (1–2), pp. 263–282.

[3] I. Ario and M. Nakazawa: Nonlinear Dynamics behavior of Multi-Folding Microstructure Systems based on Origami Skill: *Int. J. Non-Linear Mechanics*, Vol. 45(4), pp. 337–347, 2010.

[4] I. Ario and H. A. Kim: Michell Problem for the Stiffness Formation of Structural Design in 3 Dimensional Space: *Proc. of Optimizational Symposium in JSME*, 7, pp. 179–184, 2006.

[5] I. Ario: Structure with the expanding and folding equipment as a patent (No. 2006-037668), 2006.

[6] I. Ario, Y. Tanaka, M. Nakazawa, Y. Furukawa and Y. Chikahiro: Research and development of the high-efficiently foldable structure (Analysis), *Proc. of Space Structure and Material Symposium in JAXA*, Vol. 25, pp. 104–107, 2009, (in Japanese).

[7] Y. Tanaka, I. Ario, M. Nakazawa, Y. Furukawa and Y. Chikahiro: Research and development of the high-efficiently foldable structure (Experiment), *Proc. of Space Structure and Material Symposium in JAXA*, Vol. 25 pp. 108–111, 2009 (in Japanese).

[8] I. Ario, Y. Tanaka, M. Nakazawa, Y. Furukawa and Y. Chikahiro, Development of the prototype of a new emergency bridge based on the concept of optimized structure, *Journal of Structural Engineering*, *JSCE*, Vol. 64A, pp. 1–12, 2010 (in Japanese).
[9] I. Ario, Y. Furukawa, Y. Tanaka, Y. Chikahiro, S. Matumoto, M. Nakazawa, I. Tanikura and S. Ono: Dynamic Vibration of a Prototype Deployable Bridge based on MFM, *The proceedings of the 9th World Congress on Computational Mechanics and 4th Asian Pacific Congress on Computational Mechanics WCCM*/APCOM, CD, 2010.
[10] M. Nakazawa and I. Ario: Mechanical Property of Deployable Emergency Bridge Based on the Scissors Structures, *Journal of safety problems*, Vol. 5 pp. 133–138, 2010 (in Japanese).